Journal of Organometallic Chemistry 862 (2018) 13–21

Contents lists available at ScienceDirect

Journal of Organometallic Chemistry

journal homepage: www.elsevier.com/locate/jorganchem

Cyrhetrenylaniline and new organometallic phenylimines derived from 4- and 5-nitrothiophene: Synthesis, characterization, X-Ray structures, electrochemistry and *in vitro* anti-*T. brucei* activity

Patricia Toro [a], Constanza Suazo [a], Alejandra Acuña [a], Mauricio Fuentealba [a], Vania Artigas [a], Rodrigo Arancibia [b], Claudio Olea-Azar [c], Mauricio Moncada [c], Shane Wilkinson [d], A. Hugo Klahn [a, *]

[a] Instituto de Química, Pontificia Universidad Católica de Valparaíso, Casilla 4059 Valparaíso, Chile
[b] Facultad de Ciencias Químicas, Universidad de Concepción, Concepción, Chile
[c] Departamento de Química Inorgánica y Analítica, Facultad de Ciencias Químicas y Farmacéuticas, Universidad de Chile, Casilla 233, Santiago, Chile
[d] School of Biological and Chemical Sciences, Queen Mary University of London, London, United Kingdom

ARTICLE INFO

Article history:
Received 18 January 2018
Received in revised form
28 February 2018
Accepted 2 March 2018
Available online 3 March 2018

Keywords:
Organometallic Schiff bases
4-nitrothiophenecarboxaldehyde
Phenylimine bridge
Cyclic voltammetry
Anti-*Trypanosoma brucei* activity

ABSTRACT

A novel series of cyrhetrenyl (**3a**-**4a**) and ferrocenyl (**3b**-**4b**) Schiff bases were synthesized through a condensation reaction, between the known 4-ferrocenylaniline (**2b**) or the unreported 4-cyhretrenylaniline (**2a**) with 4- or 5-nitrothiophenecarboxaldehyde. The structure of **2a** and the new Schiff bases have been elucidated using conventional spectroscopic techniques (FT-IR, ^{1}H and ^{13}C NMR), mass spectrometry, and single-crystal X-ray diffraction analysis of compounds **2a**, **4a** and **3b**. Cyclic voltammetry of organometallic phenylimines derived from 5-nitrothiophene showed NO_2 group reduction potentials ($E_{1/2} \approx -0.575$ V) that were more anodic than those registered for their 4-nitro analogues ($E_{1/2} \approx -0.981$ V). All organometallic imines were tested against the bloodstream form of *Trypanosoma brucei*. Evaluation indicated that the most active complexes are the 5-nitrothiophene derivatives, **4a**, which were remarkably more active than nifurtimox. In addition, complex **4b** resulted in less toxicity to host L_6 cells than nifurtimox. The results revealed that the electronic effects of cyrhetrene and ferrocene are not an influential factor in $E_{1/2}$ and anti-*Trypanosoma brucei* activity for these new imines, which is probably due to the non-coplanarity of the [(η^5-C_5H_4)-C_6H_4-N=CH-(C_4H_2S)] system.

1. Introduction

Neglected tropical diseases (NTDs) represent a collection of infections prevalent in many regions of the developing World. They are responsible for substantial global morbidity, mortality, and economic adversity that together affect about 1 billion people worldwide [1]. One such infection is African trypanosomiasis, a debilitating condition caused by the tsetse fly-transmitted protozoan parasite *Trypanosoma brucei* (*T. brucei*) that is prevalent across sub-Saharan Africa [2]. In addition to affecting an estimated 70 million individuals living in endemic sites [2,3], this pathogen also is of veterinary and economic importance, being one of several trypanosomes responsible for a wasting disease known as Nagana in ungulate animals.

At present, pentamidine, suramin, melarsoprol and eflornithine are the only drugs available to treat the human form of the disease, although there are signficiant issues relating to toxicity, administration, the disease stage being traeted and the *T. brucei* subspecies being targeted [4]. Additionally, due to long periods of treatment, the subsequent lack of completion of the treatment course and strain variation, resistance is emerging as a major problem [5]. Recently, the WHO added nifurtimox (Nfx), a nitroheterocycle normally used against Chagas disease, to the Essential Medicines list (EML) as part of the nifurtimox-eflornithine combination therapy (NECT) for treatment of *T. brucei gambiense* [2,6]. This recommendation, together with several emerging reports on new nitroheterocyclic compounds with potential or significant *in vitro* activity against *Trypanosoma cruzi* (*T. cruzi*) and *T. brucei*, has reinvigorated interest in the use of nitroheterocyclic compounds as

* Corresponding author.
E-mail address: hugo.klahn@pucv.cl (A.H. Klahn).

https://doi.org/10.1016/j.jorganchem.2018.03.004
0022-328X/

antitrypanosomal agents [7–12].

With the aim to find new and more efficient antitrypanosomal agents, inorganic compounds containing nitroaromatic systems have also been extensively explored [13–15]. The focus has been oriented mainly toward the protozoa *T. cruzi*, the caustive agent of American trypanosomiasis (also known as Chagas Disease) and to a lesser extent to *T. brucei*. The strategy consists in the coordination of a transition metal of known pharmacological activity to the structure of a bioactive organic molecule. Based on this approach, the pioneering work of Sanchez-Delgado [16–18] and Gambino [19–21] can be cited as remarkable examples in the search for new antitrypanosomal agents. For example, some of the rhenium [19], ruthenium [20] and palladium [21] complexes with 5-nitrofuryl pharmacophore containing thiosemicarbazones as ligands have proven to be more active against *T. cruzi* than the corresponding free ligands.

In the last decades, a large number of organometallic compounds have attracted great interest because of their broad spectra of biological and pharmacological properties [22–25]. In particular, metallocene-based chemotherapeutics are known to exhibit a wide diversity of biological activity [26,27]. Among them, ferrocenyl compounds have emerged as an important research field in the ongoing discovery of metallo-therapeutic agents (i.e., antibacterial, antitumor, antimalarial, and antitrypanosomal activities) [28–31]. Promising results have been reported when targeting diseases such as cancer and malaria, indicating that the incorporation of a ferrocenyl fragment may enhance biological activities or generate new medicinal properties [32–36]. Additionally, the chemistry of cyrhetrene, [Re(η^5-C_5H_5)(CO)$_3$] (the typical example of a three-legged half-sandwich rhenium(I) complex), has undergone rapid development in the last decade [37]. Among its many other applications, this organometallic core has been recognized as a promising anticancer drug candidate [38]. For example, Re-Tamoxifen has been demonstrated to be slightly more active than Tamoxifen for the treatment of hormone-responsive breast tumors [39]. Recently, the cyrhetrenyl fragment was conjugated to sulfonamide moieties to target human carbonic anhydrases [40] and has also been incorporated into several pharmacophores for evaluation as potential antimalarial agents [41].

In recent years, our research group has been involved in the development of ferrocene and cyrhetrene derivatives bound covalently to 5-nitrofurane and 5-nitrothiophene groups as a new class of antichagasic compounds. So far, we have connected the organometallic and 5-nitro heterocyclic groups through conjugated and non-conjugated bridges. We have established the existence of a relationship between electronic effects of the organometallic fragments and the trypanocidal activities [42,43].

In view of the aforementioned potential applications of 5-nitroheterocyclic groups containing organometallic fragments, in this paper we would like to report the synthesis and characterization, including the X-ray crystallography, of an unreported cyrhetrenylaniline and a new series of bioorganometallics possessing: i) electron-donor ferrocenyl and electron-withdrawing cyrhetrenyl groups; ii) an iminophenyl bridge and, iii) a thiophene ring substituted with a nitro group in the 4- and 5-position. In addition, in the present work, we included the cyclic voltammetry studies and the anti-*T. brucei* evaluation of the Schiff bases.

2. Experimental

2.1. Materials

All manipulations were conducted under a nitrogen atmosphere using Schlenk techniques. The complexes cyrhetrene [44], 4-nitrophenylferrocene (**1b**) [45] and 4-ferrocenylaniline (**2b**) [46] were synthesized as described in the literature. Ferrocene (98%), 2-thiophenecarboxaldehyde (98%), 5-nitro-2-thiophenecarboxaldehyde (98%), 4-nitroaniline (99%), sodium nitrite (99%), hexadecyltrimethylammonium bromide (99%), *n*-BuLi 2.0 M, $ZnCl_2$ anhydrous, $PdCl_2(PPh_3)_2$ (99%), 1-bromo-4-nitrobenzene (99%), and KNO_3 (99%) were purchased from Aldrich and used as such. Solvents were obtained commercially and purified using standard methods. FT-IR spectra were recorded in solution (CH_2Cl_2) or solid state (KBr disc) on a Thermo Scientific, model Nicolet FT-IR spectrophotometer in the range of 4000-500 cm^{-1}. ^1H and ^{13}C NMR spectra were measured on a Bruker Advance 300 spectrometer using tetramethylsilane (TMS) as the internal standard and $CDCl_3$ as a solvent. The following abbreviations were used to describe the peak patterns: s = singlet, d = doublet, t = triplet, and pst = pseudo-triplet. Mass spectra were obtained on a Shimadzu model QP5050A GC-MS at the Laboratorio de Servicios Analíticos, Pontificia Universidad Católica de Valparaíso.

2.2. Synthesis of organometallic precursors

2.2.1. Synthesis of the 4-cyrhetrenylaniline (*2a*)

The preparation of the unreported 4-cyrhetrenylaniline complex was performed in two synthetic steps (Scheme 1), which involved first, a Negishi coupling reaction between cyrhetrene and 1-bromo-4-nitrobenzene and then the reduction of 4-nitrophenylcyrhetrene (**1a**).

*2.2.1.1. Synthesis of 4-nitrophenylcyrhetrene (**1a**).* *n*-BuLi (0.30 mL, 2.0 M in cyclohexane, 0.64 mmol) was added dropwise to a solution of cyrhetrene (100 mg, 0.30 mmol) in anhydrous THF (8.0 mL) at −78 °C. After that, the reaction mixture was stirred for 1.5 h at −78 °C and $ZnCl_2$ (48.0 mg, 0.35 mmol) was added. Subsequently, the mixture was allowed to warm to room temperature and was stirred for an additional 1.5 h. Then, a suspension of $PdCl_2(PPh_3)_2$ (10.0 mg, 0.014 mmol) in dry THF (2.0 mL) and a solution of 1-bromo-4-nitrobenzene ($BrC_6H_4NO_2$) (61.0 mg, 0.30 mmol) in dry THF (2.0 mL) were added to the reaction mixture and the stirring was continued, at room temperature, for 12 h. After this time, the solution was poured into water (10 mL) and extracted with dichloromethane (3 × 10 mL). The organic layers were dried over Na_2SO_4, filtered and evaporated under a vacuum. The complex (**1a**) was isolated as a pale yellow solid. The yield was 39% (45.0 mg, 0.12 mmol). IR (CH_2Cl_2, cm^{-1}): 2026, 1932 (νCO); 1523, 1349 (νNO$_2$). ^1H NMR ($CDCl_3$): δ 5.48 (t, 2H, J = 2.3 Hz, C_5H_4); 5.88 (t, 2H, J = 2.3 Hz, C_5H_4); 7.54 (d, 2H, J = 8.9 Hz, C_6H_4); 8.21 (d, 2H, J = 8.9 Hz, C_6H_4). ^{13}C NMR ($CDCl_3$): δ 83.4 (C_5H_4); 85.3 (C_5H_4); 103.4 (C_5H_{4ipso}); 124.4 (C_6H_4); 126.8 (C_6H_4); 139.3 (C_6H_4); 147.5 (C_6H_4); 193.2 (CO). Mass spectrum (based on ^{187}Re) (*m/z*): 457 [M^+]; 429 [M^+ - CO]; 401 [M^+ - 2CO]; 373 [M^+ - 3CO].

*2.2.1.2. Synthesis of 4-cyrhetrenylaniline (**2a**).* First, 4-nitrophenylcyrhetrene (**1a**) (50.0 mg, 0.13 mmol) was added to a magnetically stirred solution of concentrated hydrochloric acid

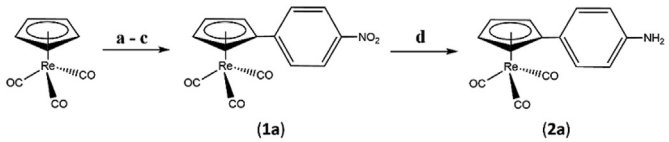

Scheme 1. Synthesis of 4-cyrhetrenylaniline (**2a**): (a) *n*-BuLi, THF, −78 °C, 1.5 h; (b) $ZnCl_2$, -78 °C, 1.5 h; (c) $PdCl_2(PPh_3)_2$, 1-bromo-4-nitrobenzene, 12 h; (d) HCl, Sn, EtOH, reflux, 4 h.

(0.40 mL) and ethanol (6.0 mL). Then granulated tin (75.0 mg, 0.63 mmol) was added and the reaction mixture was refluxed in a nitrogen atmosphere for 4 h. After cooling to room temperature, the yellow mixture that formed was treated with 3.0 mL of water and 10 mL of 0.5 M aqueous NaOH. The solid crude product was extracted with CH_2Cl_2 (2 × 20 mL), dried over Na_2SO_4, filtered and the solvent was removed in a rotary evaporator. The solid thus obtained was crystallized in a mixture with CH_2Cl_2/hexane (1:5) at −18 °C. **2a** was obtained as a dark orange solid in 47% yield (22.0 mg, 0.062 mmol). IR: (KBr, cm^{-1}) 3440, 3339 (νNH$_2$); (CH_2Cl_2, cm^{-1}) 2020, 1923 (νCO). ^{1}H NMR ($CDCl_3$): δ 3.76 (s, 2H, NH_2); 5.35 (t, 2H, J = 2.2 Hz, C_5H_4); 5.64 (t, 2H, J = 2.2 Hz, C_5H_4); 6.62 (d, 2H, J = 8.8 Hz, C_6H_4); 7.19 (d, 2H, J = 8.8 Hz, C_6H_4). ^{13}C NMR ($CDCl_3$): δ 80.3 (C_5H_4); 84.1 (C_5H_4); 111.0 (C_5H_{4ipso}); 115.1 (C_6H_4); 121.5 (C_6H_4); 127.7 (C_6H_4); 147.0 (C_6H_4); 194.6 (CO). Mass spectrum (based on ^{187}Re) (*m/z*): 427 [M^+]; 399 [M^+ - CO]; 371 [M^+ - 2CO]; 343 [M^+ - 3CO].

2.3. Synthesis of cyrhetrenyl and ferrocenyl imines. General procedure

The Schiff bases (Scheme 2) were achieved following the procedure reported by Zaheer et al. for the preparation of *N*-(arylidene)-4-ferrocenylaniline [47]. That is, 4-cyrhetrenylaniline (**2a**) or 4-ferrocenylaniline (**2b**) and equimolar amounts of the corresponding (4 or 5)-nitro-thiophene-2-carboxaldehyde were dissolved in dry ethanol (10 mL) and refluxed for 3 h in a nitrogen atmosphere. After this time, the solvent was evaporated under a vacuum and the colored solids obtained were crystallized with CH_2Cl_2/hexane (1:5) at −18 °C.

2.3.1. N-(4-nitro-2-thiophenylidene)-4-phenylcyrhetrene (**3a**)

IR (KBr, cm^{-1}): 2025 (s) (νCO), 1912 (vs) (νCO); 1617 (w) (νC = N). ^{1}H NMR ($CDCl_3$): δ 5.43 (t, 2H, J = 2.1 Hz, C_5H_4); 5.79 (t, 2H, J = 2.1 Hz, C_5H_4); 7.21 (d, 2H, J = 8.5 Hz, C_6H_4); 7.44 (d, 2H, J = 8.5 Hz, C_6H_4); 7.96 (d, 1H, J = 1.4 Hz, C_4H_2S); 8.42 (t, 1H, J = 1.4 Hz, C_4H_2S); 8.55 (s, 1H, CH=N). ^{13}C NMR ($CDCl_3$): δ 81.9 (C_5H_4); 84.7 (C_5H_4); 107.8 (C_5H_{4ipso}); 121.8 (C_6H_4); 125.5 (C_4H_2S); 127.4 (C_6H_4); 130.9 (C_4H_2S); 150.9 (CH=N); 194.1 (CO). Mass spectrum (based on ^{187}Re) (*m/z*): 566 [M^+]; 482 [M^+ - 3CO].

2.3.2. N-(5-nitro-2-thiophenylidene)-4-phenylcyrhetrene (**4a**)

The synthesis of complex **4a** was carried out similarly to that described above (general procedure); nevertheless, the reflux was prolonged for 5 h. Brown crystals, yield: 56% (27.0 mg, 0.060 mmol). IR (KBr, cm^{-1}): 2021 (s) (νCO), 1920 (vs) (νCO); 1618 (w) (νC = N). ^{1}H NMR ($CDCl_3$): δ 5.43 (t, 2H, J = 2.2 Hz, C_5H_4); 5.79 (t, 2H, J = 2.2 Hz, C_5H_4); 7.24 (d, 2H, J = 8.7 Hz, C_6H_4); 7.39 (d, 1H, J = 4.3 Hz, C_4H_2S); 7.44 (d, 2H, J = 8.7 Hz, C_6H_4); 7.91 (t, 1H, J = 4.3 Hz, C_4H_2S); 8.55 (s, 1H, CH=N). ^{13}C NMR ($CDCl_3$): δ 82.0 (C_5H_4); 84.7 (C_5H_4); 107.5 (C_5H_{4ipso}); 121.9 (C_6H_4); 127.4 (C_6H_4); 128.7 (C_4H_2S); 129.9 (C_4H_2S); 151.5 (CH=N); 194.0 (CO). Mass spectrum (based on ^{187}Re) (*m/z*): 566 [M^+]; 482 [M^+ - 3CO].

2.3.3. N-(4-nitro-2-thiophenylidene)-4-phenylferrocene (**3b**)

Red solid, yield: 53% (40.0 mg, 0.10 mmol). IR (KBr, cm-1): 1617 (w) (νC = N). ^{1}H NMR ($CDCl_3$): δ 4.05 (s, 5H, C_5H_5); 4.35 (pst, 2H, C_5H_4, J = 1.8 Hz); 4.67 (pst, 2H, C_5H_4, J = 1.8 Hz); 7.21 (d, 2H, J = 8.5 Hz, C_6H_4); 7.51 (d, 2H, J = 8.5 Hz, C_6H_4); 7.94 (d, 1H, J = 1.5 Hz, C_4H_2S); 8.40 (t, 1H, J = 1.5 Hz, C_4H2S); 8.61 (s, 1H, CH=N). ^{13}C NMR ($CDCl_3$δ 66.6 (C_5H_4); 69.4 (C_5H_4); 69.8 (C_5H_5); 121.5 (C_6H_4); 124.8 (C_4H_2S); 126.9 (C_6H_4); 130.6 (C_4H_2S); 149.3 (CH=N). Mass spectrum (*m/z*): 416 [M^+]

2.3.4. N-(5-nitro-2-thiophenylidene)-4-phenylferrocene (**4b**)

Green solid, yield: 25% (19.0 mg, 0.050 mmol). IR (KBr, cm-1): 1611 (w) (νC = N). ^{1}H NMR ($CDCl_3$): δ 4.07 (s, 5H, C_5H_5); 4.38 (pst, 2H, C_5H_4, J = 1.9 Hz); 4.70 (pst, 2H, C_5H_4, J = 1.9 Hz); 7.25 (d, 2H, J = 8.7 Hz, C_6H_4);7.39 (d, 1H, J = 4.3 Hz, C_4H_2S); 7.54 (d, 2H, J = 8.7 Hz, C_6H_4); 7.94 (d, 1H, J = 4.3 Hz, C_4H_2S); 8.64 (s, 1H, CH=N). ^{13}C NMR ($CDCl_3$): δ 66.7 (C_5H_4); 69.5 (C_5H_4); 69.9 (C_5H_5); 121.8 (C_6H_4); 126.9 (C_6H_4); 128.7 (C_4H_2S); 129.1 (C_4H_2S); 149.6 (CH=N). Mass spectrum (*m/z*): 416 [M^+]

2.4. X-ray crystal structure determinations

Single crystal X-ray diffraction studies have been successfully implemented for **2a**, **4a** and **3b**. Table 1 summarized the fundamental crystal and refinement data for the compounds. Crystals of the cyrhetrenylaniline (**2a**) and imines (**4a** and **3b**) were mounted using MiTeGen MicroMounts of a random orientation for a single crystal X-ray diffraction experiment. The compounds were studied at room temperature on a Bruker D8 QUEST diffractometer equipped with a bidimensional CMOS Photon100 detector using graphite monochromated Mo-Kα radiation. The diffraction frames were integrated using the APEX2 package [48] and were corrected for absorptions with SADABS [49]. The unit cell dimensions were determined by a least-squares fit reflection collected with I > 2s(I). Data were integrated and scaled using the APEX2 package and the scale correction was based on the equivalent reflection carried out using SADABS. The solution and refinement for compounds **2a**, **4a** and **3b** were determined using Olex2 [50]. The **2a** and **3b** structures were solved using direct methods, while the **4a** structure was solved by the Patterson Method, using ShelXS software for all the complexes [51] and a refinement package using Least Squares minimization. Calculations were performed with SMART software for data collection, while data reduction used ShelXL. The complete structures were refined using the full matrix least squares procedure on the reflection intensities (F^2) with anisotropic thermal parameters for all the nonhydrogen atoms and all the hydrogen atoms were placed in idealized locations.

2.5. Cyclic voltammetry (CV)

DMSO (spectroscopy grade) was used as a solvent and was obtained from Aldrich. Tetrabutylammonium perchlorate (TBAP), which was used as supporting electrolyte, was obtained from Fluka. CV measurements were obtained using a Metrohm 693 V A instrument with a 694 V A Stand convertor and a 693 V A Processor, in DMSO (ca. 1.0 × 10^{-3} mol L^{-1}), using TBAP (ca. 0.1 mol L^{-1}), under a nitrogen atmosphere at room temperature, using a three electrode cell. A hanging mercury drop electrode was used as the working

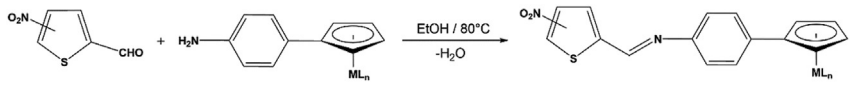

4-NO_2 ML_n = $Re(CO)_3$ (**3a**); FeCp (**3b**)
5-NO_2 ML_n = $Re(CO)_3$ (**4a**); FeCp (**4b**)

Scheme 2. Synthesis of cyrhetrenyl and ferrocenyl imines derived from 4- and 5-nitrothiophene.

Table 1
Crystal data and structure refinement results for **2a, 4a** and **3b** complexes.

Compound	**2a**	**4a**	**3b**
Empirical formula	$C_{14}H_{10}NO_3Re$	$C_{19}H_{11}N_2O_5ReS$	$C_{21}H_{16}N_2O_2SFe$
Formula weight	426.44	565.56	416.27
Temperature	296.15	296.15	296.15
Wavelength	0.71073	0.71073	0.71073
Crystal system	Orthorhombic	Triclinic	Monoclinic
Space group	Pbca	P-1	$P2_1/c$
Unit cell dimensions	a = 18.6229(6) Å α = 90.00° b = 6.1002(2) Å β = 90.00° c = 22.8140(8) Å γ = 90.00°	a = 7.3225(15) Å α = 85.171° b = 7.6762(15) Å β = 86.074° c = 16.935(3) Å γ = 76.288°	a = 22.059(4) Å α = 90.00° b = 7.3959(10) Å β = 98.851° c = 11.3482(17) Å γ = 90.00°
Volume Å^3	2591.75(15)	920.3(3)	1829.3(5)
Z	8	2	4
Density (calculated) (g/cm^3)	2.186	2.041	1.511
Absorption coefficient (mm^{-1})	9.379	6.750	0.957
F(000)	1600.0	540.0	856.0
Theta range for data collection	4.189–52.42°	4.84–54.42°	5.6–53.26°
Index ranges	$-23 \le h \le 23$, $-7 \le k \le 7$, $-28 \le l \le 28$	$-9 \le h \le 9$, $-9 \le k \le 9$, $-21 \le l \le 21$	$-27 \le h \le 27$, $-9 \le k \le 9$, $-14 \le l \le 14$
Reflections collected	105015	50340	33224
Independent reflections	2604 [R_{int} = 0.0485]	4084 [Rint = 0.0659]	3825 [R_{int} = 0.0351]
Completeness	θ = 26.2°, 99%	θ = 27.2°, 99%	θ = 26.6°, 99%
Max. and min. Transmission	T_{max} = 0.745 and T_{min} = 0.551	T_{max} = 0.700 and T_{min} = 0.562	T_{max} = 0.954 and T_{min} = 0.784
Refinement method	Least Squares minimisation.	Least Squares minimisation.	Least Squares minimisation.
Data/restraints/parameters	2604/0/180	4084/0/253	3825/0/244
Goodness-of-fit on F^2	1.188	1.084	1.034
Final R indices [I > 2 σ (*I*)]	R_1 = 0.0283, wR_2 = 0.0433	R_1 = 0.0266, wR_2 = 0.0501	R_1 = 0.0366, wR_2 = 0.0907
R indices (all data)	R_1 = 0.0387, wR_2 = 0.0450	R_1 = 0.0384, wR_2 = 0.0532	R_1 = 0.0566, wR_2 = 0.1037

electrode (HMDE), a platinum wire as the auxiliary electrode and a saturated calomel electrode (SCE) as the reference.

2.6. Biological evaluation

2.6.1. Cell culturing

L_6 rat skeletal myoblasts were grown at 37 °C under a 5% (v/v) CO_2 atmosphere in RPMI-1640 medium supplemented with 20 mM HEPES pH 7.4, 2 mM sodium glutamate, 2 mM sodium pyruvate, 2.5 U mL^{-1} penicillin, 2.5 mg mL^{-1} streptomycin and 10% (v/v) foetal calf serum (Pan Biotech UK Ltd).

T. brucei brucei BSF trypomastigotes (MITat 427 strain; clone 221a) were grown at 37 °C under a 5% (v/v) CO_2 atmosphere and cultured in HMI-9 media (Life Technologies Ltd) supplemented with 36 mM sodium bicarbonate, 0.014% (v/v) β-mercaptoethanol and 10% (v/v) heat-inactivated foetal calf serum (Pan Biotech UK Ltd) [52,53].

2.6.2. Anti-proliferative assays

The following growth inhibition assays were carried out in a 96-well plate format. L_6 rat skeletal myoblasts or *T. brucei brucei* BSF trypomastigotes were seeded at 1.0×10^4 cells mL^{-1} in 200 μL growth medium containing different concentrations of compound. The compounds were prepared in 10 mM stock solutions in 100% DMSO and stored at −20 °C. After incubation at 37 °C for 6 (L_6 cells) and 3 (*T. b. brucei*) days, resazurin (Aldrich) was added to each well at a final concentration of 12.5 μg mL^{-1} (or 2.5 μg per well). The plates were further incubated at 37 °C for 8 h (L_6 cells and *T. b. brucei*) before measuring the fluorescence of each culture using a Gemini Fluorescent Plate reader (Molecular Devices) set at λ_{EX} = 530 nm and λ_{EM} = 585 nm with a filter cut off at 550 nm. The change in fluorescence resulting from the reduction of resazurin is proportional to the number of live cells. The compound concentration that inhibits the cell growth by 50% (EC_{50}) was established using the non-linear regression tool on GraphPad Prism (GraphPad Software Inc.).

3. Results and discussion

3.1. Design and synthesis

As part of our continued interest in the study on the electronic influence of the organometallic groups into hybrid organic-organometallic imines compounds with potential antiparasitic activity, we decided to form new Schiff bases containing a [-C_6H_4-N=CH-] bridge between the organometallic entity and 4- and 5-nitro-2-thiophenyl groups. To do that we inspired on the several reports dealing with imines derived from ferrocenylanilines, which have proved to be excellent and versatile building blocks with the ability to produce several compounds with interesting electrochemical [54], antimicrobial [55–58], antioxidant [59] and antitumoral properties [60,61]. On the other hand, we selected the nitrothiophenyl group substituted into the 4- and 5-position because they allowed us to compare the reduction potential of the nitro group and the anti-*T. brucei* activity. Since ferrocenylaniline is a known compound [46,62–64], our first goal was the synthesis of the analogous cyrhetrene derivative (**2a**), which was prepared following a modified procedure reported for ferrocenylaniline. The first step involved the preparation of 4-nitrophenylcyrhetrene (**1a**) by a Negishi cross-coupling reaction between cyrhetrene and 1-bromo-4-nitrobenzene, following a strategy similar to that reported for 2-pyridylcyrhetrene [65], followed by its reduction with tin in hydrochloric acid [46] (see Scheme 1). Compound **2a** was isolated in low yield and characterized by spectroscopic and crystallographic techniques.

In the IR spectrum, **2a** showed N-H stretching absorption bands at 3440 and 3339 cm^{-1} (in KBr) which are similar to those reported for 4-ferrocenylaniline [46]. As expected, the ν(CO) bands observed at 2020 and 1923 cm^{-1} (in CH_2Cl_2) are shifted to low energy compared to the ones measured for **1a**, due to the electron-donor capability of the NH_2 group. The ^{1}H NMR spectrum of **2a** showed the resonances for the C_5 ring at 5.35 and 5.64 ppm, whereas the NH_2 and aryl hydrogen's resonances deferred by about 0.1 ppm with those reported for ferrocenylaniline [64]. The ^{13}C NMR spectra of the compound showed signals at 80.3, 84.1 and 111.0 ppm, which

is indicative of a monosubstituted cyrhetrene subunit [65]. The aromatic carbon resources were assigned by comparison of the experimental chemical shift with those measured for their ferrocenyl analogue [64]. The X-ray structure of **2a** will be discussed in the crystallography section.

To prepare the Schiff bases described below, we synthesized the unreported 4-nitro-2-thiophenecarboxaldehyde, which was prepared by nitration of thiophenecarboxaldehyde according to the procedure described by Fabrichnyi et al. [66] (Supplementary Material).

The organometallic imines derived from 4- and 5-nitrothiophene were obtained as described in Scheme 2, following the same procedure reported for some *N*-(arylidene)-4-ferrocenylaniline [58–61,67,68], that is, by the reaction of the appropriate organometallic amine (**2a** or **2b**) and the corresponding 4- or 5-nitrothiophenecarboxaldehyde in anhydrous EtOH. All compounds were isolated in low to moderate yields as pure material (by NMR), after crystallization from the CH_2Cl_2/hexane mixture. They were air stable and soluble in most common polar organic solvents, but insoluble in hexane.

In all cases, the infrared spectral analysis of these compounds showed the characteristic absorption corresponding stretching vibration of the ν(C=N) bond in the range of 1611–1618 cm^{-1} in KBr disk. Similar ν(C=N) frequency values have been previously reported for other organometallic Schiff bases derived from 5-nitrothiophene [43]. The absence of the band assigned to the aldehyde carbonyl group of nitro-heterocycle as well as the (N-H) stretching absorption of the amine precursors confirmed the formation of the organometallic imines. In addition, the cyrhetrenylimines (**3a**) and (**4a**) exhibited the characteristic ν(CO) absorption bands, in the region of 2025 and 1912 cm^{-1}.

For all complexes, the ^{1}H NMR spectra showed only the presence of a single compound. As expected, the ^{1}H NMR spectra of the ferrocenyl derivatives (**3b**) and (**4b**) exhibited a singlet at δ 4.0 and two resonances between 4.35 and 4.70 ppm, which were assigned to the protons of the ferrocenyl group. Similarly, the two resonances for the cyrhetrenyl group in compounds (**3a**) and (**4a**) were observed at identical chemical shifts (5.43 and 5.79 ppm). In all cases, the aryl hydrogen's were observed as doublets in the range 7.21–7.54 ppm. The most interesting feature of the ^{1}H NMR spectra of these Schiff bases was (i) the imine proton of the cyrhetrenyl derivatives are slightly upfield when compared to the ferrocenyl analogues, and (ii) the heterocyclic hydrogen atoms were observed in a higher field (7.94–8.42 ppm) and showed smaller coupling constants (1.4–1.5 Hz) when the nitro group was at the 4-position (**3a**-**b**) compared to their 5-substituted analogues (7.39–7.94 ppm, $J = 4.3$ Hz), meaning that they follow the same trend observed in the nitro-thiophenecarboxaldehyde precursors.

The ^{13}C NMR data also indicated the existence of a single compound. Despite that, these types of compounds could adopt two different forms (*E*- or *Z*-) and their ^{1}H and ^{13}C NMR spectra agreed with those reported for the related ferrocenyl and cyrhetrenyl Schiff bases [42,43]. This finding indicates that only one isomer (*E*-form) was present in the solution. Further proof was provided by an X-ray crystal structure determination of (**4a**) and (**3b**) (see below). The most important feature of these spectra is the presence of low field resonance (δ 149–151) assigned to the iminyl carbon. This resonance occurs at almost the same δ as those reported for other Schiff bases [55,58] and were corroborated by ^{1}H–^{13}C NMR HMQC and HSQC. It is important to note that the ^{13}C shifts of the iminyl carbons of these nitrothiophene derivatives did not show a clear dependence on the electronic properties of the organometallic substituents in the side chain and the position of the nitro group in the thiophene ring. We previously observed similar results in other imines containing 5-nitrothiophene groups [43].

3.2. X-ray crystallography

A single crystal of cyrhetrenyaniline (**2a**) was grown by slow evaporation of the CH_2Cl_2/hexane solution containing the product. The ORTEP diagram of the molecule giving its numbering scheme is shown in Fig. 1. The summary of the structural refinement data is included in Table 1 and the bond lengths and bond angles are provided as supplementary materials (Table S1). Also, **2a** was shown to crystallize in the orthorhombic crystal system showing one molecule per asymmetric unit.

The molecular structure of compound **2a** [{(η^5-C_5H_4)-(C_6H_4-4-NH_2)}Re($CO)_3$] (Fig. 1) was confirmed by X-ray diffraction studies showing the expected three-legged piano-stool structure and the presence of an aniline unit attached to the C_5H_4 ring. Average values of the Re-CO (1.907 Å) and C-O (1.146 Å) bond lengths and the Re centroid distance (1.961(2) Å) are similar to those reported for [{(η^5-C_5H_4)-2-(C_5H_4N)}Re($CO)_3$] [65]. The short C(1)-C(6) (1.473(6) Å) bond length on **2a** does suggest enhanced conjugation between the NH_2 on the phenyl and the C_5H_4 ring. This was also supported by the torsion angles (C(2)-C(1)-C(6)-C(11), 0.5(6)°), which indicate that the C_5H_4 ring and the aromatic group are almost co-planar allowing for efficient overlap of the π-electrons for bonding. Similar findings have been reported by Coville for ferrocenylaniline [62].

To compare the structural parameters of the organometallic Schiff bases with the crystallographic data reported for the related compounds [55,58,60,67], single-crystal X-ray diffraction studies were successfully carried out for [{(η^5-C_5H_4)-C_6H_4-N=CH-(C_4H_2S-5-NO_2)}Re($CO)_3$] (**4a**) and [{(η^5-C_5H_4)-C_6H_4-N=CH-(C_4H_2S-4-NO_2)}Fe(η^5-C_5H_5)] (**3b**). The molecular structures of **4a** and **3b** are shown in Figs. 2 and 3, respectively, including the selected bond lengths and bond angles. A full description of the bond lengths and bond angles are listed in Tables S2 and S3 in the Supplementary Material.

The crystallographic structures of compounds **4a** and **3b** showed that the (C_4H_2S) moiety and [(η^5-C_5H_4)-(C_6H_4)] unit are in a *trans* arrangement, thus confirming that these imines also adopt the *E* form in the solid state. In addition, for imine **3b**, the presence of the nitro group at the 4-position of thiophene was confirmed.

The cyrhetrenyl group of structure **4a** exhibited a typical three-legged piano-stool structure (Fig. 2), which is commonly observed for other half-sandwich rhenium(I) complexes studied by X-ray crystallography [43,69,70]. In **3b** (Fig. 3), the ferrocenyl fragment adopted an eclipsed conformation, similar to that found in many

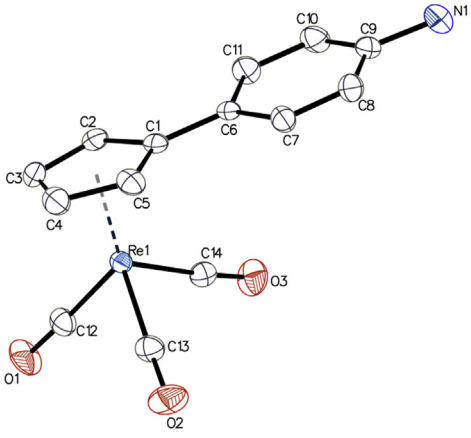

Fig. 1. Molecular structure of **2a** drawn with 30% probability displacement ellipsoids. Selected bond lengths (Å) and bond angles (°): C_5H_4(centroid)–Re 1961 (2); Re(1)–C(12) 1.895(5); Re(1)–C(13) 1.911(5); Re(1)–C(14) 1.914(5); C(1)–C(6) 1.473(6); C(9)–N(1) 1.398(7).

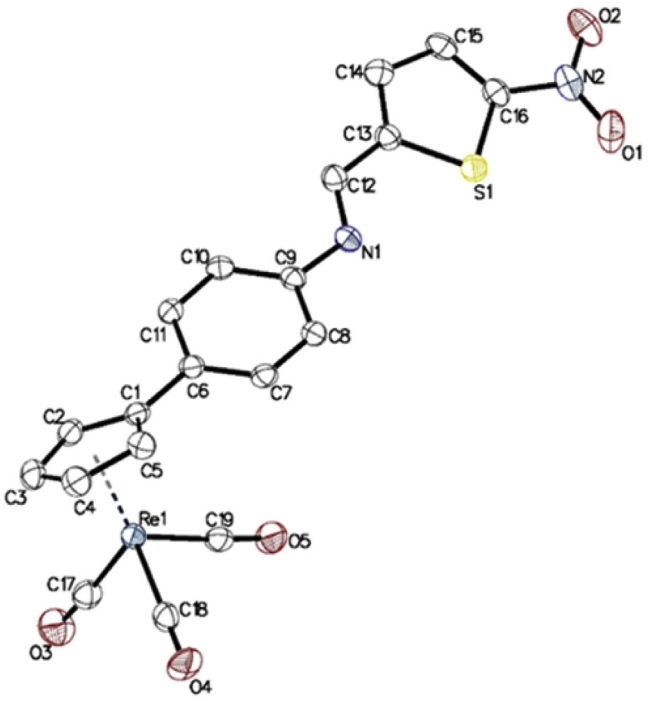

Fig. 2. Molecular structure of **4a** drawn with 30% probability displacement ellipsoids. Selected bond lengths (Å) and bond angles (°): C_5H_4(centroid)–Re 1.959(18); C(1)–C(6) 1.488(5); N(1)–C(9) 1.413(5); N(1)–C(12) 1.259(5); C(12)–C(13) 1.445(5); C(13)–C(14) 1.371(6); C(14)–C(15) 1.397(6); C(15)–C(16) 1.357(6); N(2)–C(16) 1.431(5); O(1)–N(2) 1.229(5); O(2)–N(2) 1.218(5). C(2)–C(1)–C(6) 125.9(4); C(1)–C(6)–C(11) 120.1(3); C(10)–C(9)–N(1) 124.9(4); C(9)–N(1)–C(12) 119.7(3); N(1)–C(12)–C(13) 121.7(4); C(12)–C(13)–S(1) 120.5(3).

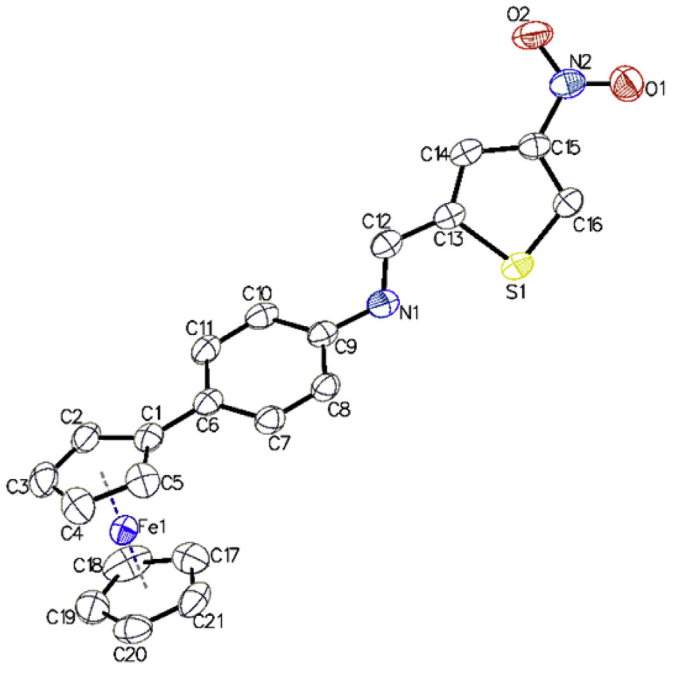

Fig. 3. Molecular structure of **3b** drawn with 30% probability displacement ellipsoids. Selected bond lengths (Å) and bond angles (°): C_5H_4(centroid)–Fe 1.6438(12), C_5H_5(centroid)–Fe 1.6487(16); C(1)–C(6) 1.469(4); N(1)–C(9) 1.412(3); N(1)–C(12) 1.268(3); C(12)–C(13) 1.440(4); C(13)–C(14) 1.359(3); C(14)–C(15) 1.406(4); C(15)–C(16) 1.350(3); N(2)–C(15) 1.463(3); O(1)–N(2) 1.214(3); O(2)–N(2) 1.218(3). C(2)–C(1)–C(6) 127.6(2); C(1)–C(6)–C(11) 122.0(2); C(10)–C(9)–N(1) 125.3(2); C(9)–N(1)–C(12) 122.3(2); N(1)–C(12)–C(13) 120.1(2); C(12)–C(13)–S(1) 118.34(18).

other monosubstituted ferrocenyl derivatives [55,71]. The distances Fe···centroid of the "C_5H_4" and "C_5H_5" rings were similar to those found for these type of compound [57,67].

The most interesting structural features of these organometallic imine compounds are: (i) in **4a** and **3b** the substituted cyclopentadienyl ring and the phenyl moiety showed a low degree of coplanarity with a dihedral angle (planes C(1)–C(5) and C(6)–C(11)) of 33.35(15)° and 17.35(11)°, respectively. Similar behaviour was found between the planes of substituted Cp and the thiophene (dihedral angles [C(1)-C(5)] and the [C(13)-C(16)-S(1)], of 51.20(16)° in **4a** and 50.02(11)° in **3b**). Therefore, an efficient electronic delocalization through the (η^5-C_5H_4-C_6H_4-C_4H_2S-NO_2) system is impeded, (ii) the torsion angle (τ) between the imine group and the nitroheterocycle fragment {[N(1)-C(12)-C(13)-S(1)] is 2.8(5)° in **4a** and 6.2(3)° in **3b**} are indicative of a high degree of coplanarity; therefore, a greater electronic delocalization can be expected between these groups, (iii) bond lengths of N(1)-C(9), N(1)-C(12) and C(1)-C(6) are similar to those reported for other Schiff bases derived from ferrocenylaniline [55,67], (iv) the iminic double bond N(1)-C(12) in **4a** (1.259(5) Å) was slightly shorter than the one measured for **3b** (1.268(4) Å), which suggests a reduced delocalization between the imine group and the heterocyclic entity in **3b**, and (v) within the nitrothiophene fragments, the bond distances [C(14)-C(15) and C(16)-N(2)] of the 5-nitrothiophene group (**4a**) are shorter than the ones found in the 4-nitro derivative (**3b**) [C(14)-C(15) and C(15)-N(2)]. This finding is probably due to a higher electronic conjugation (by resonance) between the thiophene and nitro group at the 5-position, in comparison with its 4-nitrothiophene analogue.

3.3. Electrochemical studies

To establish the possible correlation between the electronic effects of the phenylimine bridge with their $E_{1/2}$ and trypanocidal activity, we measured the reduction potentials of nitro compounds by cyclic voltammetry. The large amount of electrochemical information available in the literature for 5-nitroheterocycles (furane and thiophene) [72–74] contrasts with the limited studies dealing with nitrothiophenes and nitrofuranes nitrated in different ring positions [75]. For that reason, in this study we compared the reduction potential of 4-nitro (**3a**, **3b**) and 5-nitro (**4a**, **4b**) thienyl derivatives.

Under the recommended experimental conditions [74], the 4-nitro derivatives exhibit a different cathodic performance to that observed for their isomeric analogues (5-nitro). For example, Fig. 4 shows the comparative cyclic voltammograms of compounds **3a** and **4a**. It is important to mention that the electrochemical parameters obtained for all compounds are detailed in the Supplementary Material (Table S4).

The voltammograms obtained for 4-nitro compounds (**3a** and **3b)** show the presence of only one reduction peak with a potential near −1.0 V. This wave was correlated to an one-electron transfer process due to the reduction of the nitro group to the nitro radical anion [76a]. According to the Nicholson diagnostic criteria, a quasi-reversible reduction process should be involved [76b]. Both the shape of voltammograms and the displacement of the wave to cathodic potentials can be correlated to similar results observed by Sarragiotto and co-workers in nitro aromatic systems derived from tetrahydro-β-carbolines [76a]. On the other hand, 5-nitro derivatives (**4a** and **4b)** exhibited two reduction cathodic peaks in their voltammograms, similar to those observed in several organometallic Schiff bases derived from 5-nitrofuran and 5-nitrothiophene [42,43]. The first one, observed at −0.65 V, was attributed to the nitro/nitro-radical anion couple [74,77] (comparatively lower than those obtained for 4-nitro derivatives).

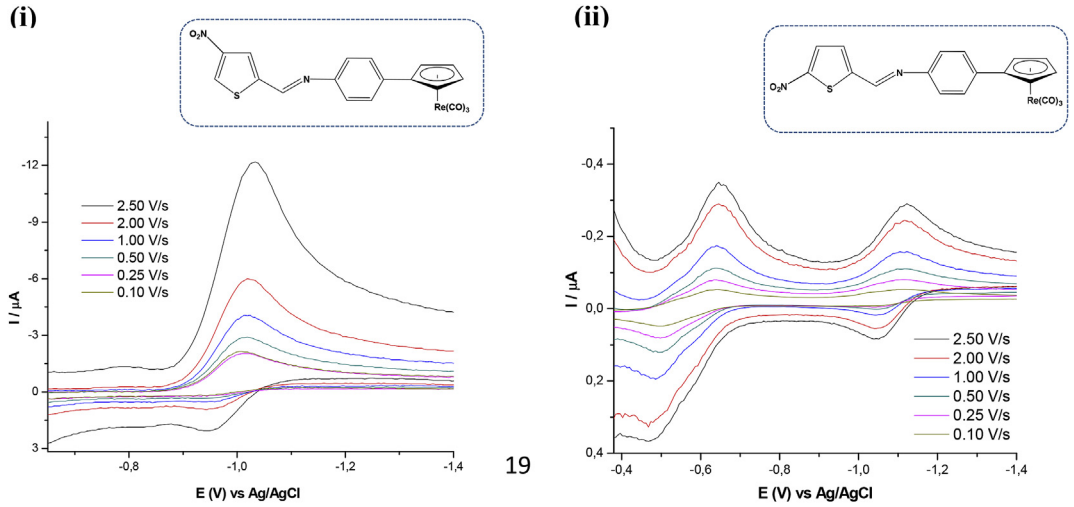

Fig. 4. (i) Cyclic voltammogram of compounds **3a** and (ii) Cyclic voltammogram of compounds **4a** in DMSO of 0.1–2.5 V^{-1}.

According to the standard reversibility criteria, this couple corresponded to a reversible diffusion-controlled single electron transfer. The second irreversible peak displayed a more negative reduction potential (≈ -1.1 V), which was assigned to the electroreduction of the nitro-radical anion to form a hydroxylamine derivative (this reduction wave is not observed in the 4-nitro derivatives in the potential range used) [77].

Taking into account the electrochemical behaviour for all the compounds, it is possible to make some general conclusions: (i) in the two series of compounds (4-nitro and 5-nitro) the $E_{1/2}$ values [$E_{1/2} = (Ea + Ec)/2$] (Table 2) did not correlated with the electronic nature of the organometallic fragment attached to the phenylimine bridge, suggesting that there is no electronic communication between the two substituents of the imine group, which is probably due to the lack of planarity of the phenylimine bridge with the organometallic and nitrothiopene groups (see crystallographic section) and, (ii) 5-nitro derivatives exhibited lower $E_{1/2}$ values than nifurtimox and 4-nitroderivatives, under the same conditions, indicating that these compounds had a better ability to generate radical species [74]. These results are in agreement with the studies (DFT calculations, cyclic voltammetry and electrochemical electron spin resonance spectroscopy) performed by Spinelli et al. on nitrothiophenes [75].

3.4. *In vitro anti-T. brucei activity*

To evaluate the anti-trypanosomal activity by modifying the position of the nitro group attached to the thiophene ring (4-NO_2 and 5-NO_2), we undertook an *in vitro* growth inhibitory study of all the compounds against *T. brucei brucei* BSF trypomastigotes and rat skeletal myoblasts (L_6 cells) using standard drug screens. From the resultant dose-response curves (cell viability (%) vs Log[compound]), the EC_{50} values in µM were determined for all organometallic imines. The EC_{50} values are provided in Table 2 and compared against the standard antiparasitic drug Nfx as a control.

From the data depicted in Table 2, some general observations can be achieved. Firstly, there was not a linear correlation between the nitro-reduction ($E_{1/2}$) with the anti-*T. brucei* activity (EC_{50}). Similar results have been previously reported for related nitrothiophene compounds with antichagasic activity [43]. Second, 5-nitrothiophenes are more efficient anti-*T. brucei* agents ($EC_{50} = 0.44$ for **4a** and $EC_{50} = 2.72$ µM for **4b**) than their 4-nitro analogues ($EC_{50} = 16.32$ for **3a** and 9.77 µM for **3b**). These results are probably related to the generation (in agreement with the electrochemical results) and a better stabilization of the anion nitro radical (NO_2_) in the biological target [5,11,78–80]. Third, the cyrhetrenyl derivative containing the 5-nitrothiophene (**4a**) was a more potent trypanocidal agent than the ferrocenyl analogue (**4b**) possibly due to the better lipophilicity of the cyrhetrenyl compared to ferrocenyl fragment [41b]. Four, independent of the substitution on the thiophene ring, the cyrhetreny derivatives (**3a** and **4a**) showed comparable cytotoxicity, whereas the ferrocenyl containing the 5-nitrothiophenyl ring (**4b**) is less cytotoxic than its 4-nitro analogue (**3b**) and nifurtimox. Lastly, the Selectivity Index (SI)

Table 2
In vitro anti-*T. brucei* activity, cytotoxicity in L_6 cells, selectivity index and reduction potentials of cyrhetrenyl (**3a**, **4a**) and ferrocenyl (**3b**, **4b**) imines.

Compound	Structrure	EC_{50} (µM)[a] ± SE[b] for:		Selectivity Index[c]	$E_{1/2}$ (V)[d] (NO_2 group)
		T. brucei	L_6	L_6/*T. b. brucei*	
3a	4-NO_2	16.32 ± 1.72	20.77 ± 3.71	1.27	−0.980
4a	5-NO_2	0.44 ± 0.01	13.27 ± 1.58	30.2	−0.560
3b	4-NO_2	9.77 ± 1.21	9.22 ± 1.90	0.94	−0.985
4b	5-NO_2	2.72 ± 0.45	>150	>55.1	−0.590
Nfx	5-NO_2	3.65 ± 0.16	88.67 ± 3.49	24.3	−0.880[e]

Nfx: nifurtimox.
[a] EC_{50}: concentration that inhibits 50% of growth. Values shown are the average of four or more experiments.
[b] Standard error (SE).
[c] The selectivity index was calculated as a ratio of the [EC_{50} L_6 cells: EC_{50} *T b. brucei*].
[d] $E_{1/2}$: ($E_{pc} + E_{pa}$)/2.
[e] Data From Ref. [74].

calculated as the ratio between the EC_{50} values of L_6 cell and *T. brucei* (Table 2) demonstrated that the organometallic compounds derived from 5-nitrothiophene, **4a** and **4b**, (SI = 30.2 and > 55, respectively) have improved selectivity against the parasite than nifurtimox (SI = 24.3). Therefore, these new organometallic compounds could represent a promising family for the design of novel anti-*T. brucei* agents.

4. Conclusion

New organometallic phenylimines derived from 4- and 5-nitrothiophene were synthesized and characterized. Like many other organometallic Schiff bases, these compounds adopt an *anti*-configuration for the iminyl fragment in solution and in the solid state. Cyclic voltammetry studies demonstrated that phenylimines derived from 5-nitrothiophene presented reduction potentials of the NO_2 group ($E_{1/2} \approx -0.575$ V) that were more anodic than those registered for their 4-nitro analogues ($E_{1/2} \approx -0.982$ V) and nifurtimox ($E_{1/2} = -0.880$ V). Evaluation of the *in vitro* activity against *Trypanosoma brucei* indicated that the most active complexes are those possessing the 5-nitrothiophene moiety, such as **4a**, which is 8-fold more active than nifurtimox, whereas complex **4b** was more active and less toxic to host L_6 cells than nifurtimox. The non-coplanarity of the [(η^5-C_5H_4)-C_6H_4-N=CH-(C_4H_2S)] system impeded the fluid electronic communication between the cyrhetrenyl and ferrocenyl fragments with the nitrothiophene groups. Accordingly, the electronic effects of the organometallic units are not influential factors in $E_{1/2}$ and the anti-*Trypanosoma brucei* activity of these compounds.

Acknowledgments

A.H.K and R.A acknowledge FONDECYT-Chile (Project, 1150601, 11130443) and FONDEQUIP (Projects EQM 130154 and 120095). P.T. acknowledges CONICYT (Chile) for a graduate fellowship (21130293) and D.I. Pontificia Universidad Católica de Valparaíso for a scholarship.

Appendix A. Supplementary data

CCDC 1586086-1586088 contains the supplementary crystallographic data for this paper. These data can be obtained free of charge from the Cambridge Crystallographic Data Centre, 12 Union Road, Cambridge CB2 1EZ, UK; fax: (+44) 1223-336-033; or by e-mail: deposit@ccdc.cam.ac.uk.

Appendix B. Supplementary data

Supplementary data related to this article can be found at https://doi.org/10.1016/j.jorganchem.2018.03.004.

References

[1] http://www.who.int/neglected_diseases/diseases/en/(consulted 20/11/2017).
[2] http://www.who.int/mediacentre/factsheets/fs259/en/(consulted 20/11/2017).
[3] R. Brun, J. Blum, F. Chappuis, C. Burri, Lancet 375 (2010) 148.
[4] M.P. Barrett, D.W. Boykin, R. Brun, R.R. Tidwell, Br. J. Pharmacol. 152 (2007) 1155.
[5] S.R. Wilkinson, J.M. Kelly, Expet Rev. Mol. Med. 11 (2009) 31.
[6] O. Yun, G. Priotto, J. Tong, L. Flevaud, F. Chappuis, PLoS Neglected Trop. Dis. 4 (2010) e720.
[7] M.V. Papadopoulou, W.D. Bloomer, H.S. Rosenzweig, I.P. O'Shea, S.R. Wilkinson, M. Kaiser, Eur. J. Med. Chem. 103 (2015) 325.
[8] M.V. Papadopoulou, W.D. Bloomer, H.S. Rosenzweig, S.R. Wilkinson, J. Szular, M. Kaiser, Eur. J. Med. Chem. 117 (2016) 179.
[9] M. Kaiser, M.A. Bray, M. Cal, B.B. Trunz, E. Torreele, R. Brun, Antimicrob. Agents Chemother. 55 (2011) 5602.
[10] C. Fonseca-Berzal, A. Ibáñez-Escribano, F. Reviriego, J. Cumella, P. Morales, N. Jagerovic, J.J. Nogal-Ruiz, J.A. Escario, P.B. da Silva, MdeN. Soeiro, A. Gómez-Barrio, V.J. Arán, Eur. J. Med. Chem. 115 (2016) 295.
[11] C. Bot, B.S. Hall, G. Álvarez, R. Di Maio, M. González, H. Cerecetto, S.R. Wilkinson, Antimicrob. Agents Chemother. 57 (2013) 1638.
[12] M.N. Balfour, C.H. Franco, C.B. Moraes, L.H. Freitas-Junior, H.A. Stefani, Eur. J. Med. Chem. 128 (2017) 202.
[13] a) M. Fernández, E. Rodríguez Arce, C. Sarniguet, T.S. Morais, A.I. Tomaz, C. Olea Azar, R. Figueroa, J.D. Maya, A. Medeiros, M. Comini, M.H. Garcia, L. Otero, D. Gambino, J. Inorg. Biochem. 153 (2015) 306;
b) E. Rodríguez Arce, I. Machado, B. Rodríguez, M. Lapier, M.C. Zúñiga, J.D. Maya, C. Olea Azar, L. Otero, D. Gambino, J. Inorg. Biochem. 170 (2017) 125.
[14] M. Vieites, L. Otero, D. Santos, J. Toloza, R. Figueroa, E. Norambuena, C. Olea-Azar, G. Aguirre, H. Cerecetto, M. González, A. Morello, J.D. Maya, B. Garat, D. Gambino, J. Inorg. Biochem. 102 (2008) 1033.
[15] M. Vieites, P. Smircich, M. Pagano, L. Otero, F. Luane Fischer, H. Terenzi, M.J. Prieto, V. Moreno, B. Garat, D. Gambino, J. Inorg. Biochem. 105 (2011) 1704.
[16] R. Sánchez Delgado, K. Lazardi, L. Rincón, J. Urbina, J. Med. Chem. 36 (1993) 2041.
[17] M. Navarro, T. Lehman, E. Cisneros-Fajardo, A. Fuentes, R. Sánchez Delgado, J. Urbina, Polyhedron 19 (2000) 2319.
[18] R. Sánchez Delgado, M. Navarro, K. Lazardi, R. Atencio, M. Caparelli, F. Vargas, J. Urbina, A. Boulliez, A. Noels, D. Masi, Inorg. Chim. Acta. 275–276 (1998) 528.
[19] L. Otero, G. Aguirre, L. Boiani, A. Denicola, C. Rigol, C. Olea-Azar, J.D. Maya, A. Morello, M. González, D. Gambino, H. Cerecetto, Eur. J. Med. Chem. 41 (2006) 1231.
[20] L. Otero, P. Noblia, D. Gambino, H. Cerecetto, M. Gonzalez, J.A. Ellena, O.E. Piro, Inorg. Chim. Acta. 344 (2003) 85.
[21] L. Otero, M. Vieites, L. Boiani, A. Denicola, C. Rigol, L. Opazo, C. Olea-Azar, J.D. Maya, A. Morello, R.L. Krauth-Siegel, O.E. Piro, E. Castellano, M. González, D. Gambino, H. Cerecetto, J. Med. Chem. 49 (2006) 3322.
[22] G. Jaouen, Bioorganometallics: Biomolecules, Labeling, Medicine, Wiley-Vch, 2006.
[23] P. Stepnicka (Ed.), Ferrocene. Ligands, Materials and Biomolecules, Wiley, Weinheim, Germany, 2008.
[24] E. Alessio, Bioinorganic Medicinal Chemistry, John Wiley & Sons, 2011.
[25] G. Jaouen, N. Netzler-Nolte, Medicinal Organometallic Chemistry (In Topics in Organometallic Chemistry, Vol. 32), Spinger, 2010.
[26] C.G. Hartinger, P.J. Dyson, Chem. Soc. Rev. 38 (2009) 391.
[27] A. Monney, M. Albrecht, Coord. Chem. Rev. 257 (2013) 2420.
[28] M. Patra, G. Gasser, N. Metzler-Nolte, Dalton Trans. 41 (2012) 6350.
[29] S.S. Braga, A.M.S. Silva, Organometallics 32 (2013) 5626.
[30] M. Navarro, W. Castro, C. Biot, Organometallics 31 (2012) 5715.
[31] K. Kowalski, Ł. Szczupk, S. Saloman, D. Steverding, A. Jabłoński, V. Vrček, A. Hildebrandt, H. Lang, A. Rybarczyk-Pirek, Chem. Plus. Chem. 82 (2017) 303.
[32] J.J. Cázares-Marinero, O. Buriez, E. Labbe, S. Top, C. Amatore, G. Jaouen, Organometallics 32 (2013) 5926.
[33] J.J. Cázares-Marinero, S. Top, G. Jaouen, J. Organomet. Chem. 751 (2014) 610.
[34] S. Top, A. Vessières, G. Leclercq, J. Quivy, J. Tang, J. Vaissermann, M. Huché, G. Jaouen, Chem. Eur J. 9 (2003) 5223.
[35] C. Biot, D. Taramelli, I. Forfar-Bares, L.A. Maciejewki, M. Boyce, G. Nowogroscki, J.S. Brocard, N. Basilico, P. Olliaro, T. Egan, Mol. Pharm. 2 (2005) 185.
[36] C. Supan, G. Mombo-Ngoma, M.P. Dal-Bianco, C.L. Ospina Salazar, S. Issifou, F. Mazuir, A. Flali-Ansary, C. Biot, D. Ter-Minassian, M. Ramharter, P.G. Kresner, B. Lell, Antimicrob. Agents Chemother. 56 (2012) 3165.
[37] A. Leonidova, G. Gasser, ACS Chem. Biol. 9 (2014) 2180.
[38] G. Jaouen, S. Top, A. Vessières, P. Pigeon, G. Leclercq, L. Laios, Chem. Commun. (2001) 383.
[39] A. Vessières, P. Pigeon, M.-N. Rager, M. Huchè, E. Salomon, C. Cabestaing, J. Vaissermann, G. Jaouen, Chembiochem 5 (2004) 1104.
[40] D. Can, B. Spingler, P. Schmutz, F. Mendes, P. Raposinho, C. Fernandes, F. Carta, A. Innocenti, I. Santos, C.T. Supuran, R. Alberto, Angew. Chem. Int. Ed. Engl. 51 (2012) 3354.
[41] a) P. Toro, A.H. Klahn, B. Pradines, F. Lahoz, A. Pascual, C. Biot, R. Arancibia, Inorg. Chem. Commun. 35 (2013) 126;
b) R. Arancibia, F. Dubar, B. Pradines, I. Forfar, D. Dive, A.H. Klahn, C. Biot, Bioorg. Med. Chem. 18 (2010) 8085.
[42] R. Arancibia, A.H. Klahn, G.E. Buono-Core, E. Gutierrez-Puebla, A. Monge, M.E. Medina, C. Olea-Azar, J.D. Maya, F. Godoy, J. Organomet. Chem. 696 (2011) 3238.
[43] R. Arancibia, A.H. Klahn, G.E. Buono-Core, D. Contreras, G. Barriga, C. Olea-Azar, M. Lapier, J.D. Maya, A. Ibañez, M.T. Garland, J. Organomet. Chem. 743 (2013) 49.
[44] F. Agbossou, E.J. O'Connor, C.M. Garner, N. Quirós Méndez, J.M. Fernández, A.T. Patton, J.A. Ramsden, J.A. Gladysz, J.M. O'Connor, T. Tajima, K.P. Gable, Inorg. Synth. 29 (1992) 21.
[45] P. Hu, K.-Q. Zhao, H.-B. Xu, Molecules 6 (2001) M249.
[46] H. Ping, K.Q. Zhao, H.B. Xu, Molecules 6 (2001) M250.
[47] M. Zaheer, A. Shah, Z. Akhter, R. Qureshi, B. Mirza, M. Tauseef, M. Bolte, Appl. Organomet. Chem. 25 (2010) 61.
[48] SAINT (v8.27A), Bruker Analytical X-Ray Systems Inc, Madison, WI, USA, 2012.
[49] G.M. Sheldrick, SADABS, (Version 2.05), Bruker Analytical X-Ray Systems Inc,

Madison, WI, USA, 2012.
[50] O.V. Dolomanov, L.J. Bourhis, R.J. Gildea, J.A.K. Howard, H. Puschmann, J. Appl. Crystallogr. 42 (2009) 339.
[51] G.M. Sheldrick, Acta. Cryst. A64 (2008) 112.
[52] H. Hirumi, K. Hirumi, J. Parasitol. 75 (1989) 985.
[53] S. Alsford, T. Kawahara, L. Glover, D. Horn, Mol. Biochem. Parasitol. 144 (2005) 142.
[54] B. Shaabani, Z. Shaghaghi, Tetrahedron 66 (2010) 3259.
[55] E.M. Njogu, B. Omondi, V.O. Nyamori, S. Afr, J. Chem. 69 (2016) 51.
[56] M.K. Rauf, R. Gul, Z. Rashid, A. Badshah, M.N. Tahir, M. Shahid, A. Khan, Spectrochim. Acta Mol. Biomol. Spectrosc. 136 (2015) 1099.
[57] R. Gul, M.K. Rauf, A. Badshah, S.S. Azam, M.N. Tahir, A. Khan, Eur. J. Med. Chem. 85 (2014) 438.
[58] M. Zaheer, A. Shah, Z. Akhter, R. Qureshi, B. Mirza, M. Tauseef, M. Bolte, Appl. Organometal. Chem. 25 (2011) 61.
[59] R.A. Hussain, A. Badshash, M. Sohail, B. Lal, A.A. Altaf, Inorg. Chim. Acta. 402 (2013) 133.
[60] M. Shabbir, Z. Akhter, I. Ahmad, S. Ahmed, M. Bolte, H. Ismail, B. Mirza, Inorg. Chim. Acta. 463 (2017) 102.
[61] H. Nawaz, Z. Akhter, S. Yameen, H.M. Siddiqi, B. Mirza, A. Rifat, J. Organomet. Chem. 694 (2009) 2198.
[62] E.N. Nxumalo, V.O. Nyamori, N.J. Coville, J. Organomet. Chem. 693 (2008) 2942.
[63] C. Gautier, O. Ghodbane, D.D.M. Wayner, D. Bélanger, Electrochim. Acta 54 (2009) 6327.
[64] A.A. Altaf, N. Khan, A. Badshah, B. Lal, Shafiqullah S. Anwar, M. Subhan, J. Chem. Soc. Pak. 33 (2011) 691.
[65] T. Cautivo, H. Klahn, F. Godoy, C. López, M. Font-Bardía, T. Calvet, E. Gutierrez-Puebla, A. Monge, Organometallics 30 (2011) 5578.
[66] B.P. Fabrichnyi, S.M. Kostrova, G.P. Gromova, Y.L. Gol`dfarb, Khim. Geterotsikl. Soedin. 11 (1973) 1483.
[67] B.X. Ye, Y. Xu, F. Wang, Y. Fu, M.P. Song, Inorg. Chem. Commun. 8 (2005) 44.
[68] J. Razumiene, A. Vilkanauskyte, V. Gureviciene, V. Laurinavicius, N.V. Roznyatovskaya, Y.V. Ageeva, M.D. Reshetova, A.D. Ryabov, J. Organomet. Chem. 668 (2003) 83.
[69] J. Gómez, A.H. Klahn, M. Fuentealba, D. Sierra, C. Olea-Azar, J.D. Maya, M.E. Medina, J. Organomet. Chem. 839 (2017) 108.
[70] C. Quintana, G. Silva, A.H. Klahn, V. Artigas, M. Fuentealba, C. Biot, I. Halloum, L. Kremer, N. Novoa, R. Arancibia, Polyhedron 134 (2017) 166.
[71] C. López, R. Bosque, J. Arias, E. Evangelio, X. Solans, M. Font-Bardía, J. Organomet. Chem. 672 (2003) 34.
[72] J. Argüello Da Silva, L.J. Núñez Vergara, S. Bollo, J.A. Squella, J. Electroanal. Chem. 591 (2006) 99.
[73] C.M. Aravena, A.C. Olea, H. Cerecetto, M. González, J.D. Maya, J. Rodríguez-Becerra, Spectrochim. Acta Mol. Biomol. Spectrosc. 79 (2011) 312.
[74] C. Olea-Azar, A.M. Atria, F. Mendizabal, R. Di Maio, G. Seoane, H. Cerecetto, Spectrosc. Lett. 31 (1998) 99.
[75] C. Boga, M. Calvaresi, P. Franchi, M. Lucarini, S. Fazzini, D. Spinelli, D. Tonelli, Org. Biomol. Chem. 10 (2012) 7986.
[76] a) L.T. Tonin, V.A. Barbosa, C.C. Bocca, E.R. Ramos, C.V. Nakamura, W.F. da Costa, E.A. Basso, T.U. Nakamura, M.H. Sarragiotto, Eur. J. Med. Chem. 44 (2009) 1745;
b) R.S. Nicholson, I. Shain, Anal. Chem. 36 (1964) 706.
[77] C. Olea-Azar, C. Rigol, F. Mendizabal, A. Morello, J.D. Maya, C. Moncada, E. Cabrera, R.D. Maio, M. González, H. Cerecetto, Free Rad. Res. 37 (2003) 993.
[78] B.S. Hall, C. Bot, S.R. Wilkinson, J. Biol. Chem. 286 (2011) 13088.
[79] W. Apt, Drug Des. Devel. Ther. 4 (2010) 243.
[80] R. Viotti, C. Vigliano, B. Lococo, M. Alvarez, M. Petti, G. Bertocchi, A. Armenti, Expert Rev. Anti Infect. Ther. 7 (2009) 157.